EXCAVATION OF THE MANTLE IN BASIN-FORMING EVENTS ON THE MOON. Katarina Miljkovic[1], Mark A. Wieczorek[1], Gareth S. Collins[2], Sean C. Solomon[3], David E. Smith[4], Maria T. Zuber[4]. [1]Institut de Physique du Globe de Paris, Sorbonne Paris Cité, Université Paris Diderot, France (email: miljkovic@ipgp.fr). [2]Department of Earth Sciences and Engineering, Imperial College London, UK. [3]Lamont-Doherty Earth Observatory, Columbia University, Palisades, NY 10963, USA; and Department of Terrestrial Magnetism, Carnegie Institution of Washington, Washington, DC 20015, USA [4]Department of Earth, Atmospheric and Planetary Sciences, Massachusetts Institute of Technology, Cambridge, MA 02139, USA.

Introduction: The Moon is a differentiated body composed of a geochemically distinct crust, mantle and core. Analysis of lunar basalts indicates that the mantle is composed predominantly of the minerals olivine and pyroxene, in contrast to the crust that is composed mostly of anorthite [e.g., 1]. Direct sampling of the lunar mantle, or observation of mantle exposures on the surface from orbit, would provide important constraints towards understanding not only early differentiation processes, but also the mechanism by which the Moon formed.

Previous numerical simulations of the basin forming process showed that a substantial amount of mantle should have been excavated by the largest impact basins [2-6], but such material is lacking in the lunar sample collection. Recent global crustal thickness maps of the Moon, derived from gravity measurements obtained by NASA's Gravity Recovery and Interior Laboratory (GRAIL) mission [7], show that the crust is thinner than previously thought. With an average thickness between 34 and 43 km [8], it is now even more probable that portions of the mantle were excavated during the largest impact events.

Remote sensing data collected by the spectral profiler on the Kaguya spacecraft have recently indicated regions on the lunar surface with high abundances of olivine [9], a mineral that could be representative of Moon's upper mantle material. The most prominent of these detections surround the Crisium impact basin on the nearside and the Moscoviense basin on the farside (Figure 1). GRAIL-derived crustal thickness maps show that these two basins have a crustal thickness approaching zero at their centers, supporting the interpretation [9] that the mantle of the Moon was excavated during the formation of these basins.

Method: We used the iSALE-2D hydrocode to simulate basin formation, with pre-impact crustal thicknesses between 30 and 60 km and target temperatures representative of the epoch when lunar basins formed [10]. The nearside basins were modeled in a hot crust and farside basins in a cold crust, as described earlier [2]. We investigated the impact conditions under which the mantle is exposed on the surface, and where such exposures should be found. GRAIL-derived crustal thickness profiles of basins were used to validate the numerical impact simulations, and the locations of excavated mantle were compared with the Kaguya olivine detections.

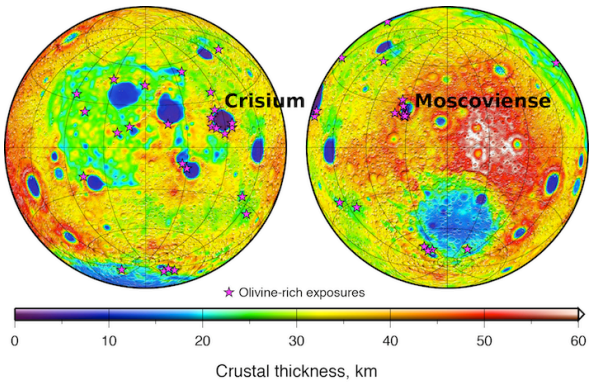

Figure 1. Crustal thickness of the Moon derived from GRAIL gravity data [8], and locations of olivine-rich exposures detected by Kaguya (red stars) [9].

Results: The Crisium impact was modeled using a 60-km projectile impacting the Moon vertically at 17 km/s. The numerical simulation, shown in black lines in the upper panel of Figure 2, produced a basin with a crustal thinning diameter of 480 km, which compares closely to the GRAIL value of 500 km. The simulation shows that mantle materials are predicted to be exposed not only in the central portion of the basin but also over a portion of the crust just exterior to the region of crustal thinning. The mare fill in Crisium (denoted by dark orange) has a radius of about 238 km and covers most, but not all, of the predicted mantle exposures. Two small craters that formed after mare emplacement (Picard and Pierce) may have excavated through these mare basalts and into the underlying mantle [12].

In the simulation, nearly all of the impact melt consists of mantle material (<1.5% of crustal materials are distributed in the melt pool). Although the iSALE-2D profiles are shown 2 hours after impact, the GRAIL data show the basin as observed today. Long-term viscous flow is expected to cause the basin to rebound a few kilometers [11].

Whether mantle material is exposed on the surface of the Moon after an impact depends upon the impact and target conditions. Numerical modeling shows that for the same impact conditions, and in targets with the same crustal thickness, impact basins form differently depending on whether the target is hot or cold [2]. Basins formed in a hotter target have a weaker crust, which allows the crust to flow more easily back toward the basin center than in the case of a cold crust. For

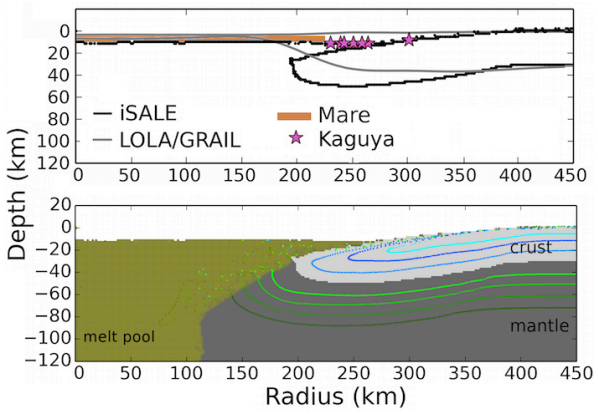

Figure 2. (top) Surface elevation and crust-mantle interface (gray lines) from Lunar Orbiter Laser Altimeter and GRAIL data, compared to numerical results. (bottom) Basin structure from iSALE-2D showing location and extent of the impact melt pool (>50% melt), mantle uplift and crustal overturn (as shown by the blue tracers in the crust and green tracers in the mantle).

this reason, it is less likely that mantle materials will be exposed if the target is hot.

A suite of iSALE-2D simulations was performed to determine the conditions required to expose mantle materials. Figures 3 and 4 show these results as a function of the pre-impact crustal thickness and the diameter of crustal thinning beneath the basin. In these figures, red represents the parameter space where mantle material should be exposed. A hot temperature profile representative of the nearside was used in Figure 3, whereas a cold temperature profile representative of the farside was used in Figure 4 [2, 10]. As expected, as the pre-impact crustal thickness decreases, and as the final basin size increases, it becomes easier to excavate and expose mantle materials on the surface.

The diameters and pre-impact crustal thicknesses of GRAIL-observed basins on the nearside and farside are plotted in Figures 3 and 4, respectively. These figures demonstrate that the mantle should have been excavated by the largest basins on the nearside and that the majority of these (Imbrium, Serenitatis, Crisium, Nectaris, Humorum, Humboldtianum) are associated with olivine-rich exposures. On the farside, Orientale and Moscoviense are predicted to be have excavated the mantle, from which only Moscoviense is associated with prominent olivine-rich exposures. Although Orientale is not associated with olivine-rich materials, this basin formed on the limb of the Moon, and given its proximity to the Procellarum KREEP Terrane, it might be better treated as having formed in a hot crust representative of the nearside. According to the exposure threshold shown in Figure 3, Orientale would not then be expected to have exposed mantle materials during its formation.

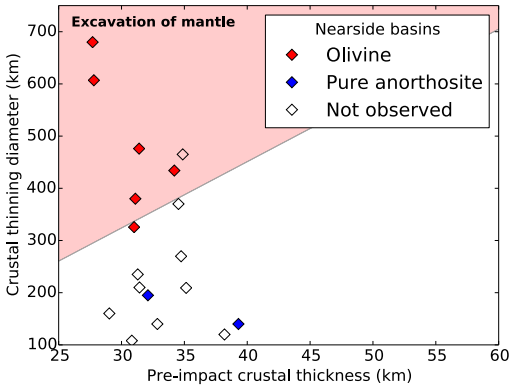

Figure 3. The upper half of this image (red shading) denotes the range of impact conditions that should have led to the excavation of mantle materials on the nearside hemisphere of the Moon. Symbols denote actual basins from GRAIL data; red symbols indicate an association with olivine-rich materials, and blue an association with pure anorthosite [9, 13]. Unfilled symbols denote basins where neither was detected.

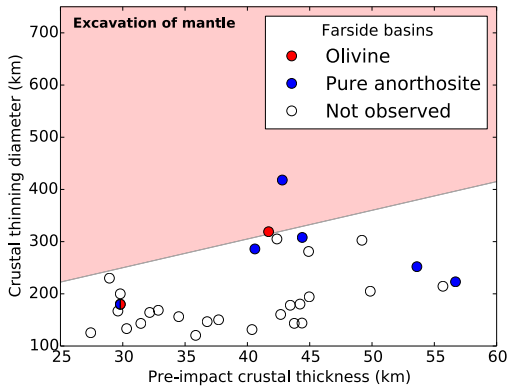

Figure 4. Same as Figure 3, but for impact basins that formed in a cold crust, on the farside of the Moon.

Conclusions: Our numerical work suggests the largest basins on the nearside and the Moscoviense basin on the farside could have excavated through the crust and exposed mantle materials at the surface. These results support the interpretation [9] that olivine-rich deposits adjacent to impact basins could have been derived from the lunar mantle.

References: [1] Wieczorek, M. A. et al. (2006) *Rev. Mineral. Geochem.* 60, 221-364. [2] Miljkovic, K. et al. (2013) *Science* 342, 724-726. [3] Ivanov, B. A. (2007) *LPS*, 38, abstract 2003. [4] Stewart, S. T. (2011) *LPS*, 42, abstract 1633. [5] Potter, R. W. K. et al (2012) *GRL* 39, L18203. [6] Potter, R. W. K. et al. (2012) *Icarus* 220, 730-743. [7] Zuber, M. T. et al. (2013) *Science* 287, 1788-1793. [8] Wieczorek, M. A. et al. (2013) *Science* 339, 671-675. [9] Yamamoto, S. et al. (2010) *Nature Geosci.* 3, 533-536. [10] Laneuville, M. et al. (2013) *J. Geophys. Res.* 118, 1435-1452. [11] Melosh, H. J. et al. (2013) *Science* 340, 1552-1555. [12] Wieczorek, M. A. and Phillips, R. J. (1998) *J. Geophys. Res.* 103, 1715-1724. [13] Nakamura, R. et al. (2013) *LPS*, 44, abstract 1988.